Science Advances
AAAS

Supplementary Materials for

Piezoelectric ultrasound energy–harvesting device for deep brain stimulation and analgesia applications

Tao Zhang, Huageng Liang, Zhen Wang, Chaorui Qiu, Yuan Bo Peng, Xinyu Zhu, Jiapu Li, Xu Ge, Jianbo Xu, Xian Huang, Junwei Tong, Jun Ou-Yang, Xiaofei Yang, Fei Li*, Benpeng Zhu*

*Corresponding author. Email: benpengzhu@hust.edu.cn (B.Z.); ful5@xjtu.edu.cn (F.L.)

Published 15 April 2022, *Sci. Adv.* **8**, eabk0159 (2022)
DOI: 10.1126/sciadv.abk0159

The PDF file includes:

Figs. S1 to S19
Tables S1 to S7
Note S1
Legends for movies S1 to S9

Other Supplementary Material for this manuscript includes the following:

Movies S1 to S9

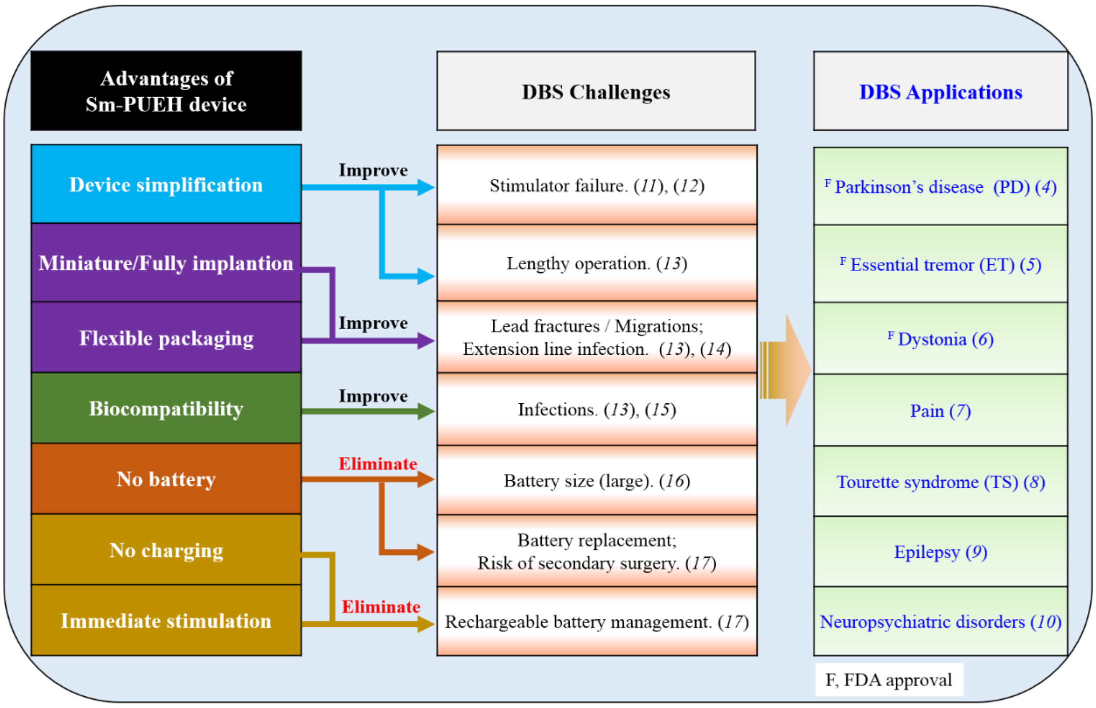

Fig. S1. The summary of DBS. DBS applications, challenges proposed, as well as the advantages of this work in dealing with the specific DBS challenges (thin arrows).

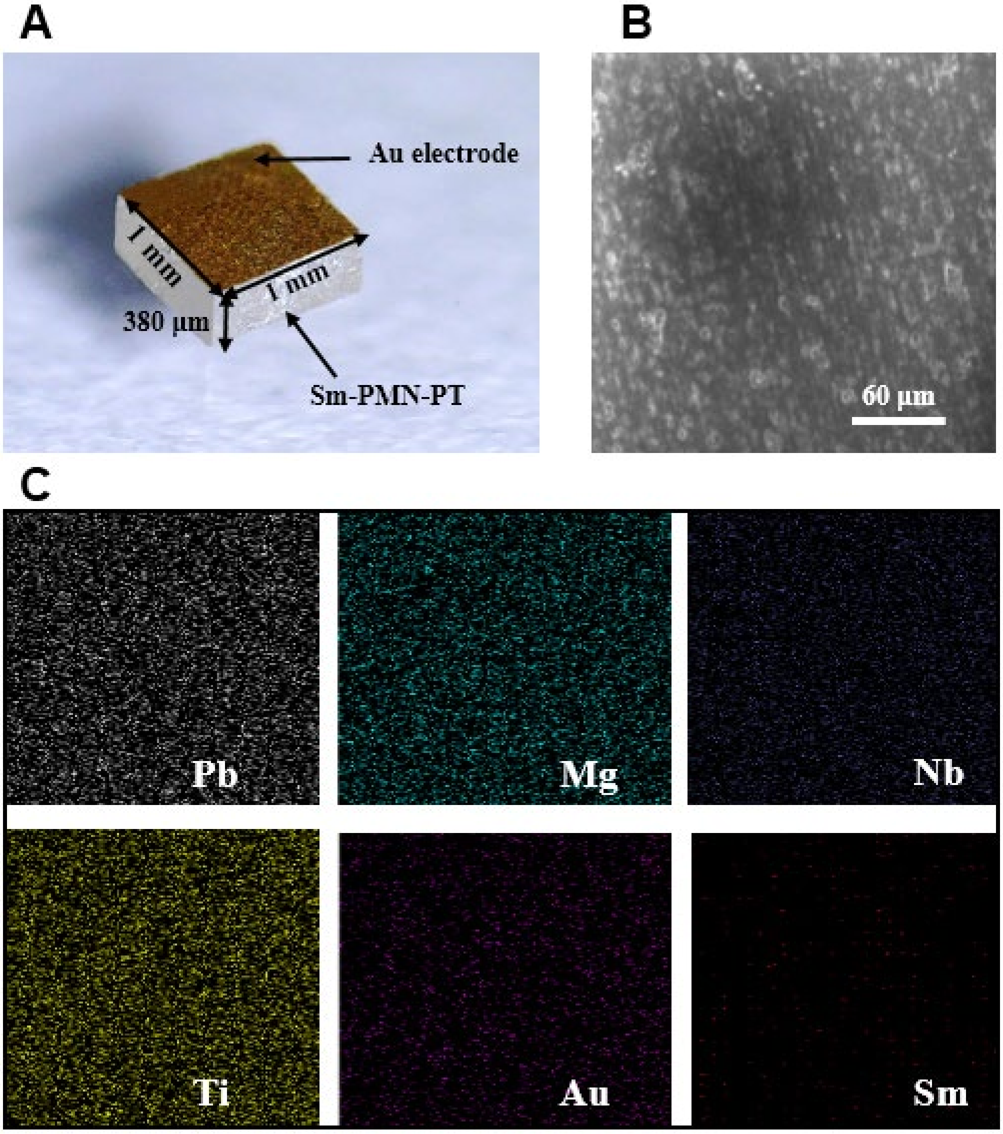

Fig. S2. Characterization of single Sm-PMN-PT element. (A) Photo of one element (Sm-PMN-PT). **(B)** An enlarged view of the surface of one element. **(C)** Energy dispersive spectroscopy (EDS) elemental mapping images for one element.

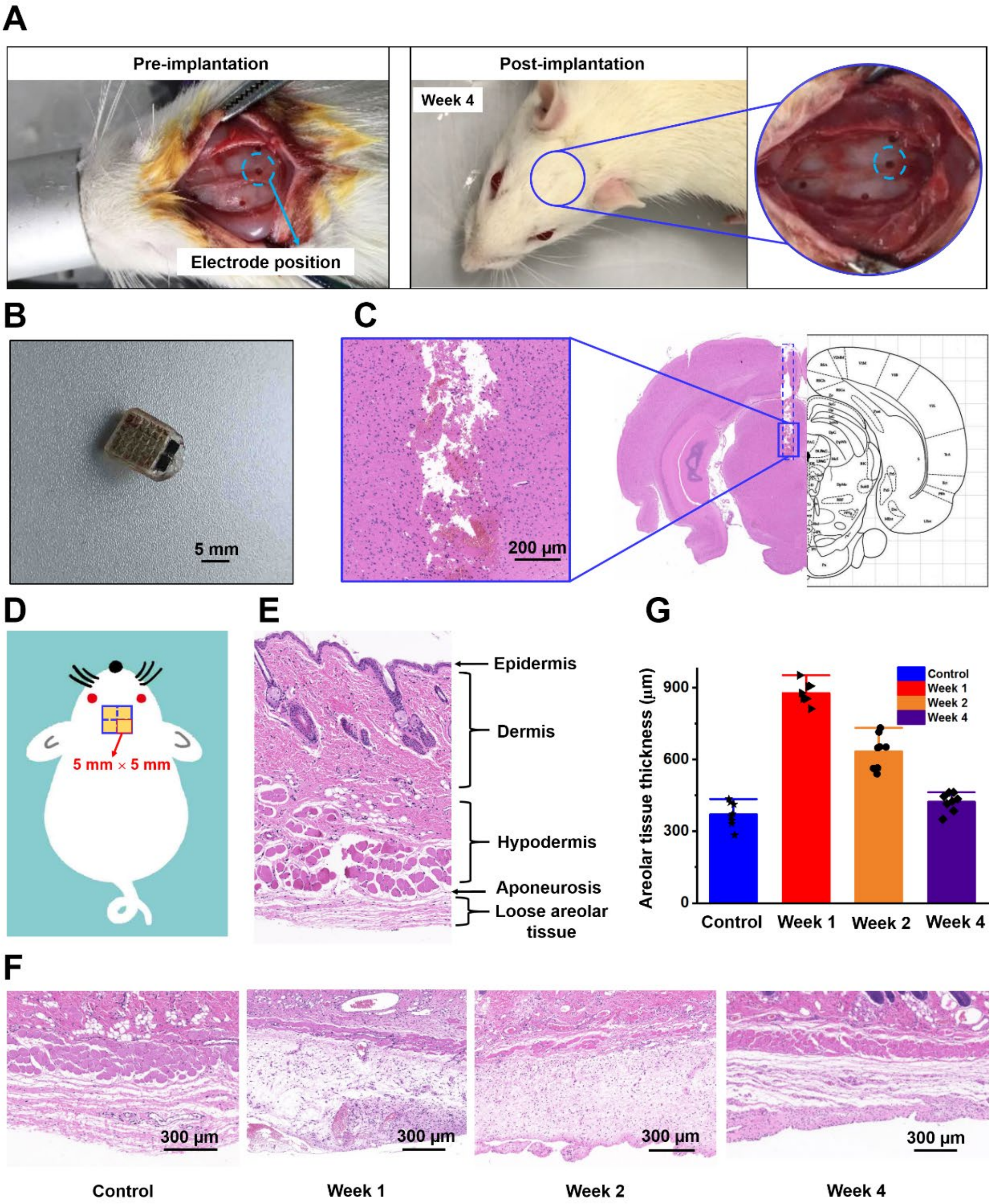

Fig. S3. Biocompatibility studies for the fully implantable Sm-PUEH device. (A) Rat scalp status of pre-implantation and post-implantation (4 weeks). **(B)** The removed Sm-PUEH device. **(C)** Representative H & E stained brain image of electrode track without obvious tissue damage. **(D)** Schematic diagram of a rat showing where tissues were taken. **(E)** Representative skin tissues stained with H & E. **(F)** Representative H & E stained skin tissue images obtained at 1 week, 2 weeks and 4 weeks after surgery with Sm-PUEH device and a normal skin tissue image (control). **(G)** Analysis of loose areolar tissue thicknesses, indicating the rats gradually recovered.

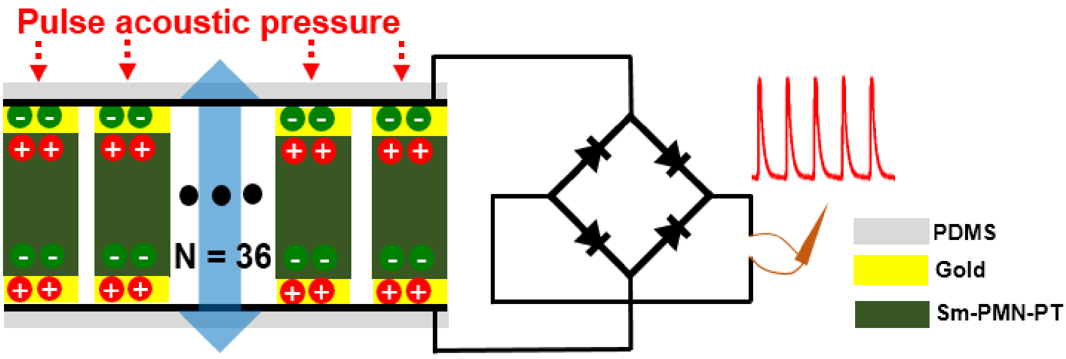

Fig. S4. The circuit diagram of Sm-PUEH device.

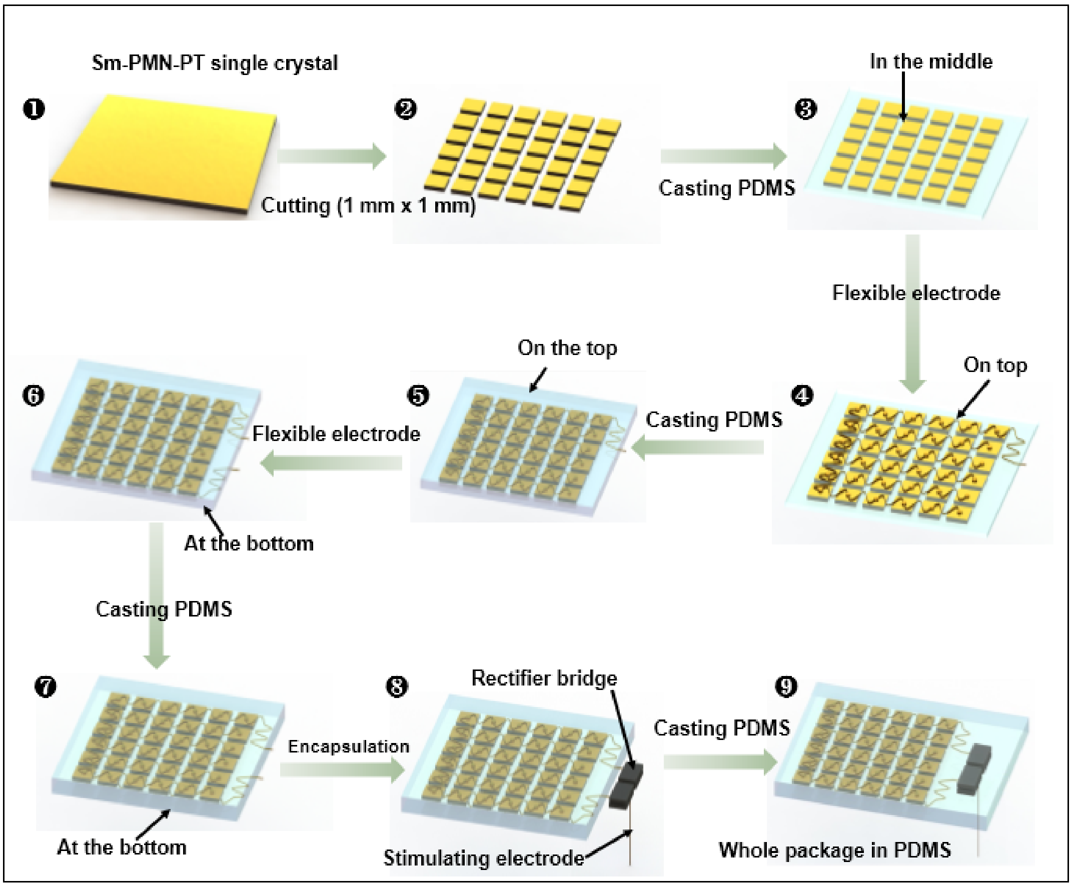

Fig. S5. Flow chart of Sm-PUEH device fabrication process.

Fig. S6. Size and mass measurement for Sm-PUEH device.

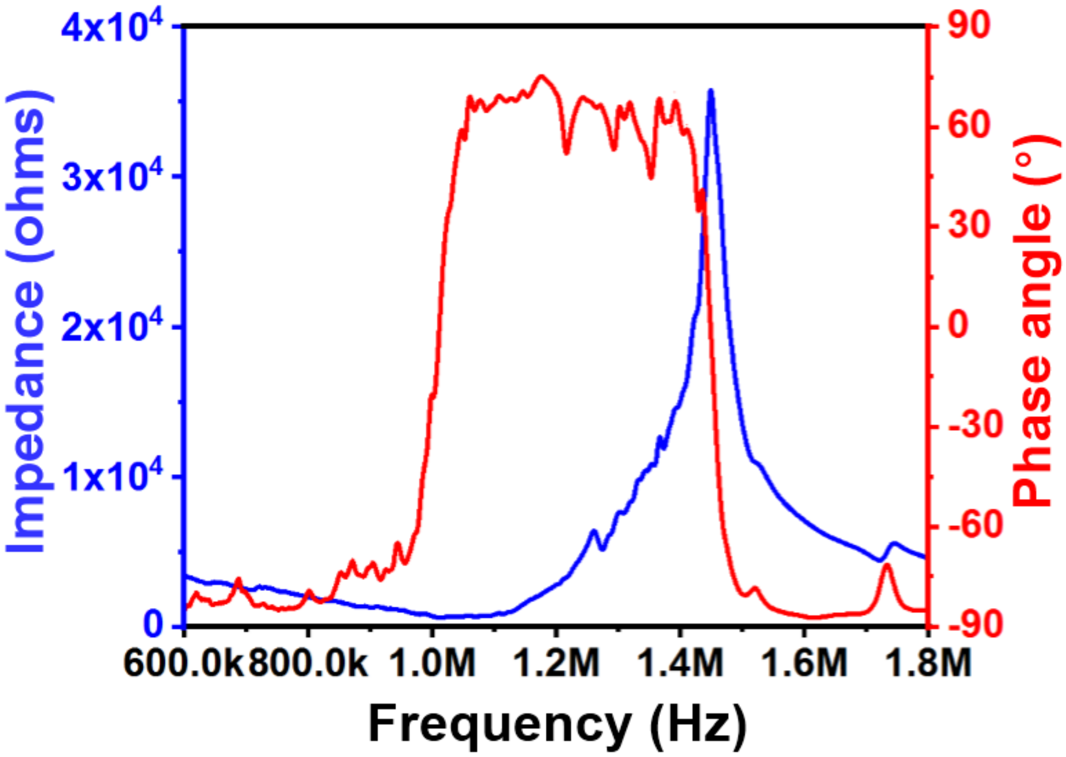

Fig. S7. Electrical impedance and phase angle of one Sm-PMN-PT element.

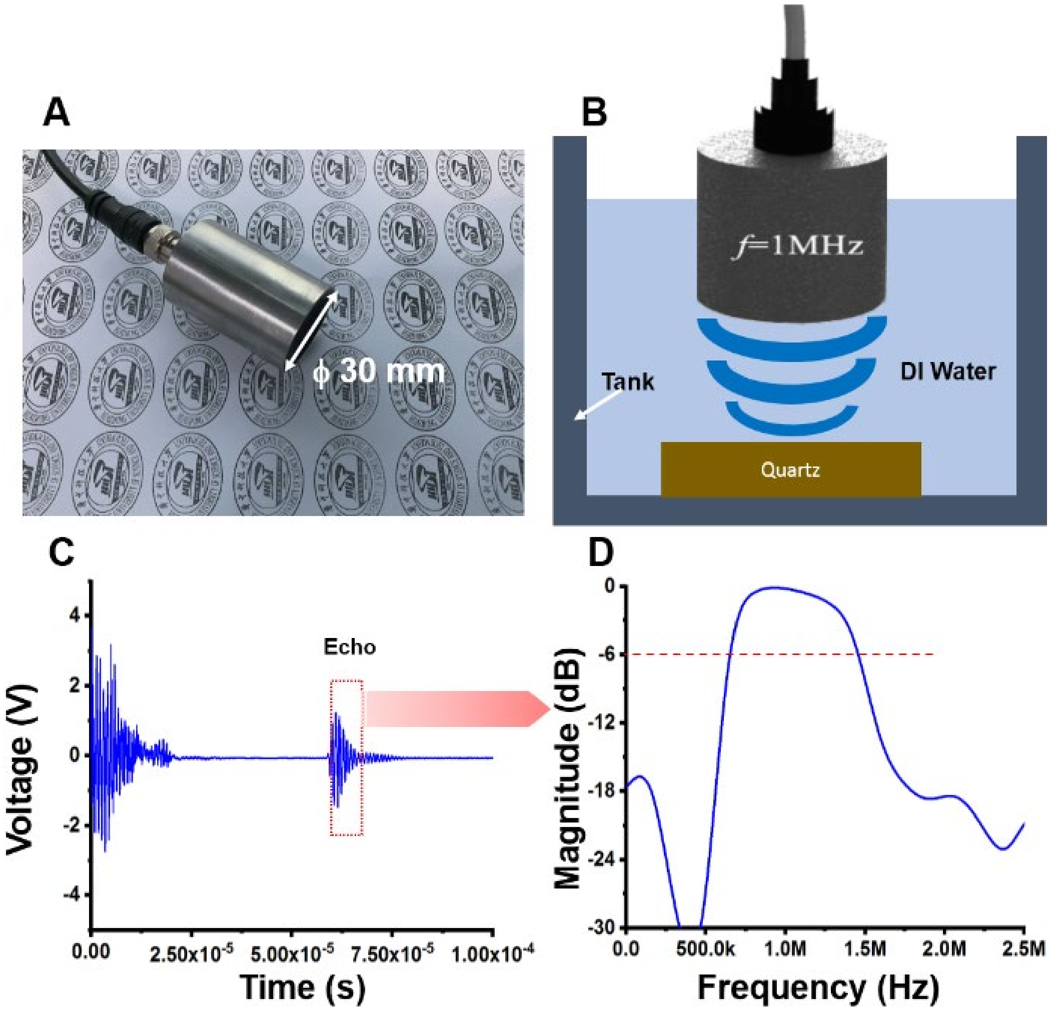

Fig. S8. Characterization of ultrasound transducer used in this study. (A) 1 MHz ultrasound transducer (diameter-30 mm) in this work. **(B)** The experimental diagram of the transducer echo test. **(C)** The echo signal of the transducer. **(D)** The frequency gain diagram of the echo signal.

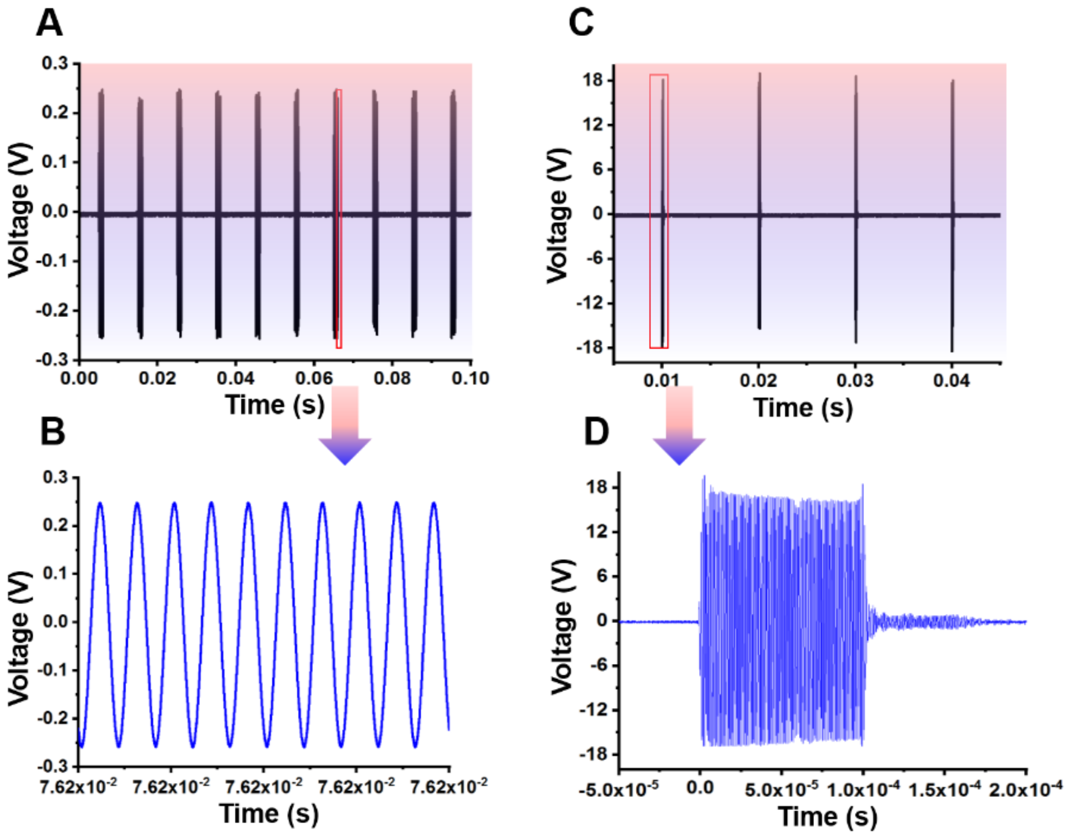

Fig. S9. Excitation signal and output signal of Sm-PUEH device. (A) Excitation signal of the signal source. **(B)** Partial enlargement of **Fig. S9-A. (C)** Output voltage signal of Sm-PUEH device. **(D)** Partial enlargement of output voltage signal of **Fig. S9-C**.

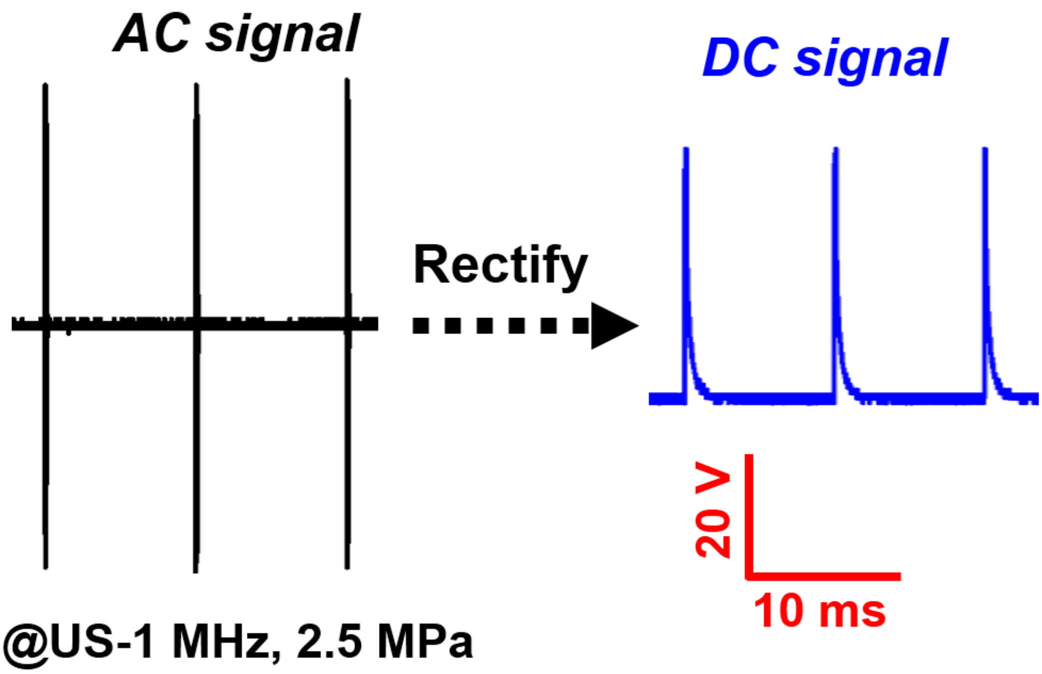

Fig. S10. The AC/DC converting of the output voltage by rectifier circuit.

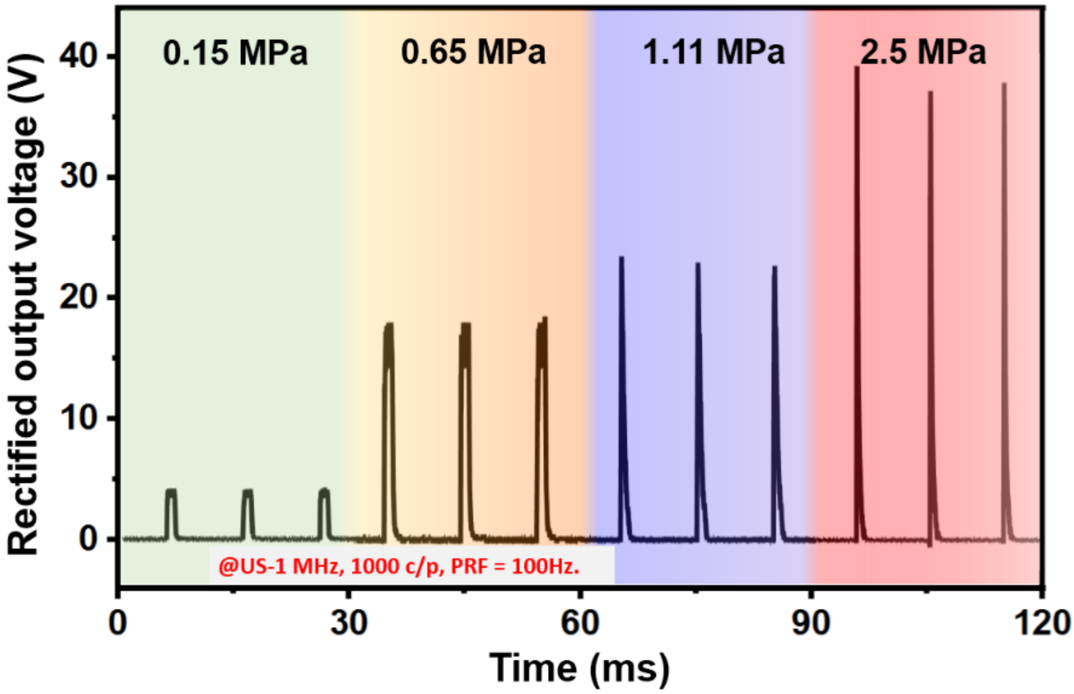

Fig. S11. The rectified output voltage signals of Sm-PUEH device under different ultrasound intensities.

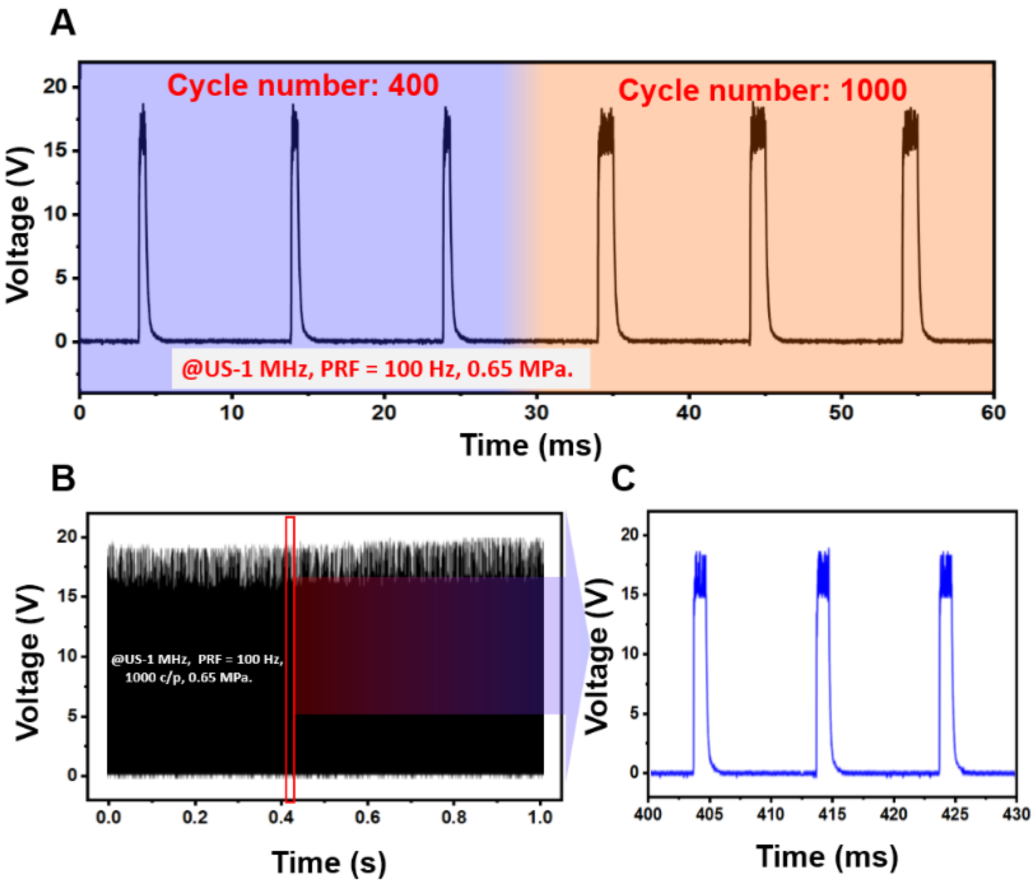

Fig. S12. Rectified output voltage signals of Sm-PUEH device. (A) Rectified output voltage signals of Sm-PUEH device with different ultrasound cycle number. **(B)** The stability of output voltage (1 s). **(C)** Partial enlargement in **(B)**-diagram.

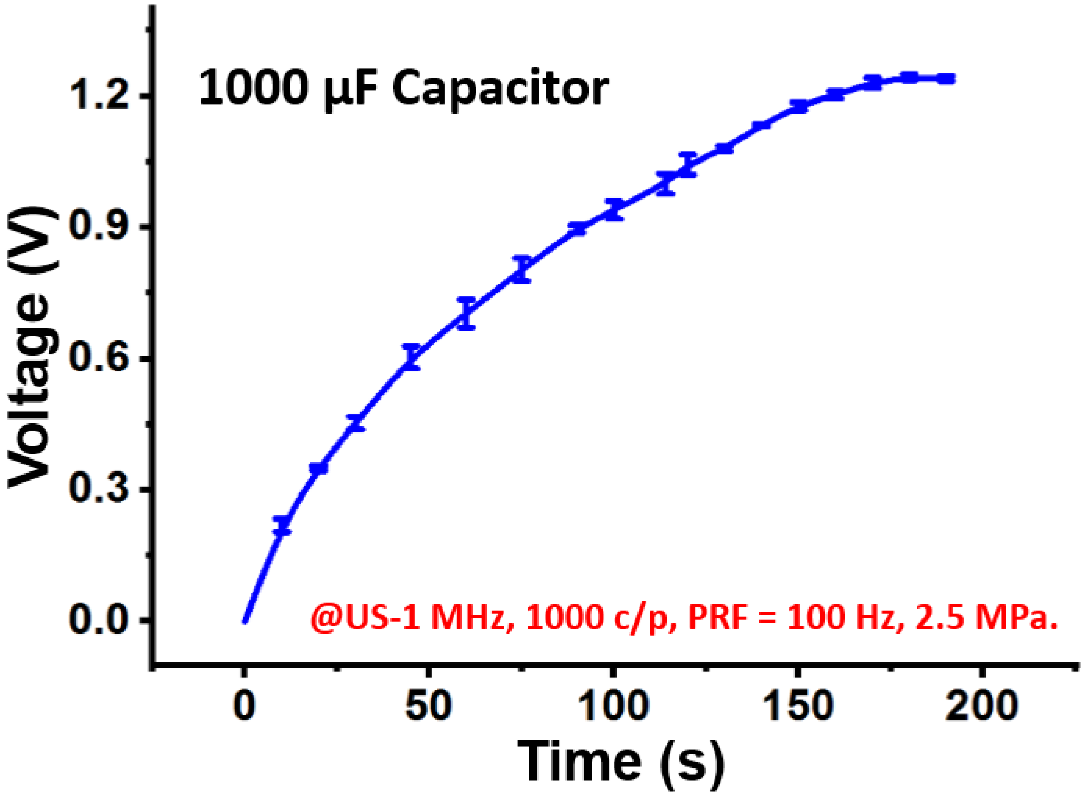

Fig. S13. Charging curve of a capacitor (1000 μF) using Sm-PUEH device. The charging voltage reaches the saturation value of 1.25 V within 180 s.

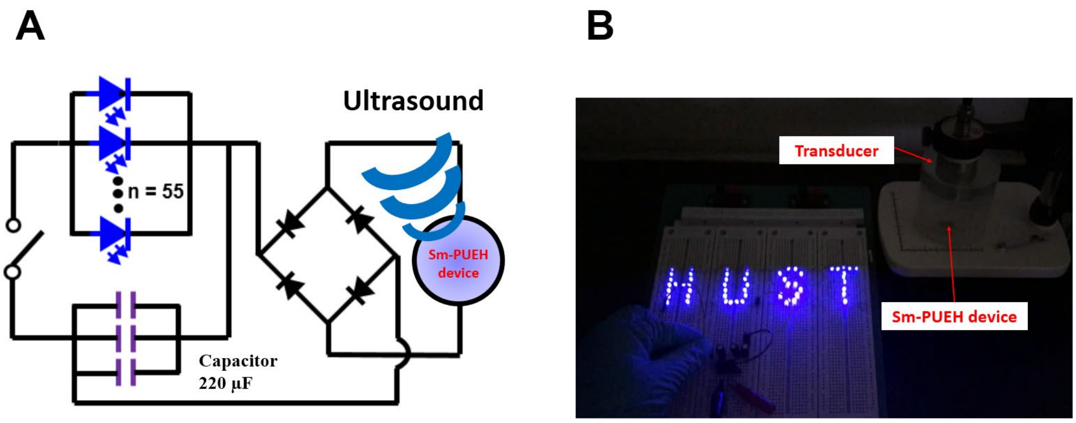

Fig. S14. Lighting application of Sm-PUEH device after long-time charging. (A) Schematic diagram for lighting experiment. **(B)** Lighting of 55 blue LEDs with "***HUST***" pattern after three 220 µF capacitors charged by Sm-PUEH device under an applied ultrasound (US–1 MHz, 1000 c/p, PRF = 100 Hz, 2.5 MPa) for five minutes.

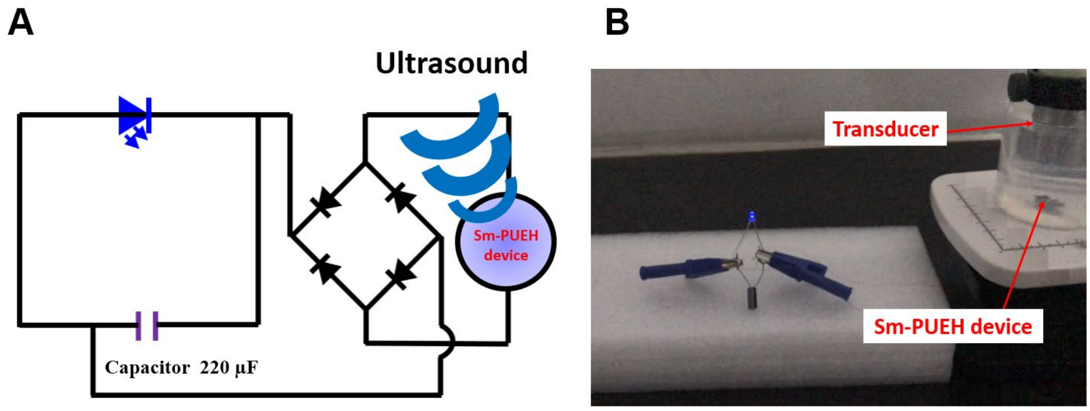

Fig. S15. Lighting application of Sm-PUEH device after short-time charging. (A) Schematic diagram for lighting experiment. **(B)** Instant lighting of one blue LED connected with a 220 μF capacitor in parallel charged by Sm-PUEH device under an applied ultrasound (US–1 MHz, 1000 c/p, PRF = 100Hz, 2.5 MPa).

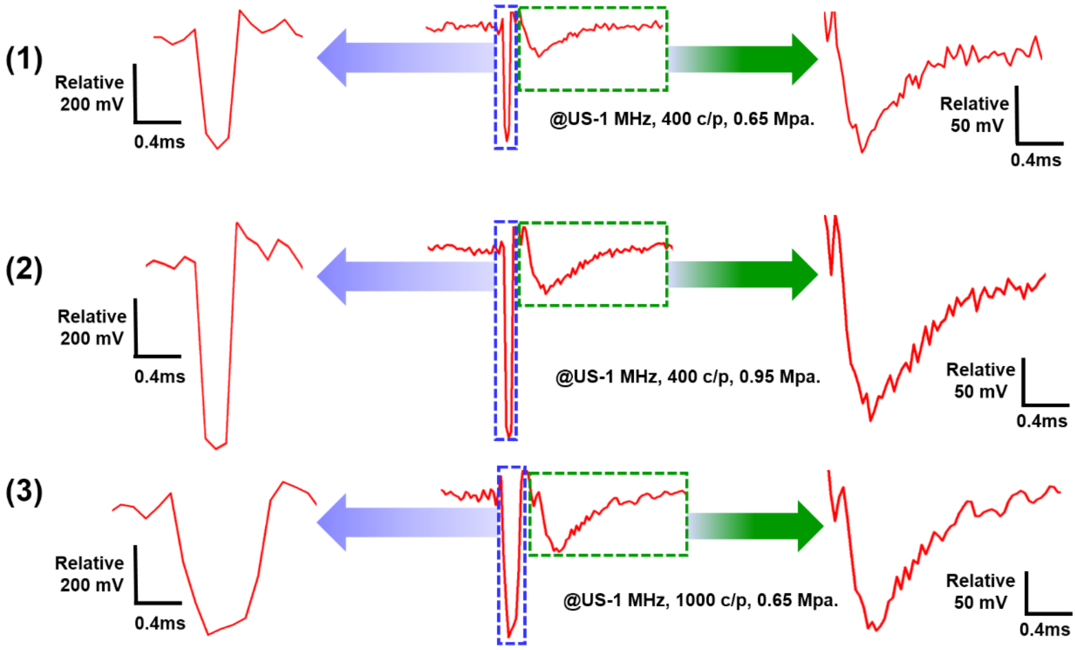

Fig. S16. The Changes of recorded signals with different stimulating conditions. The signal in the middle column is the combined signal, where the blue arrow indicates the stimulated signal and the green one is the recorded signal. When the stimulated signal's amplitude is increased (2) or its duration is elevated (3), the amplitude of the recorded signal is enhanced, meanwhile its waveform has no obvious change.

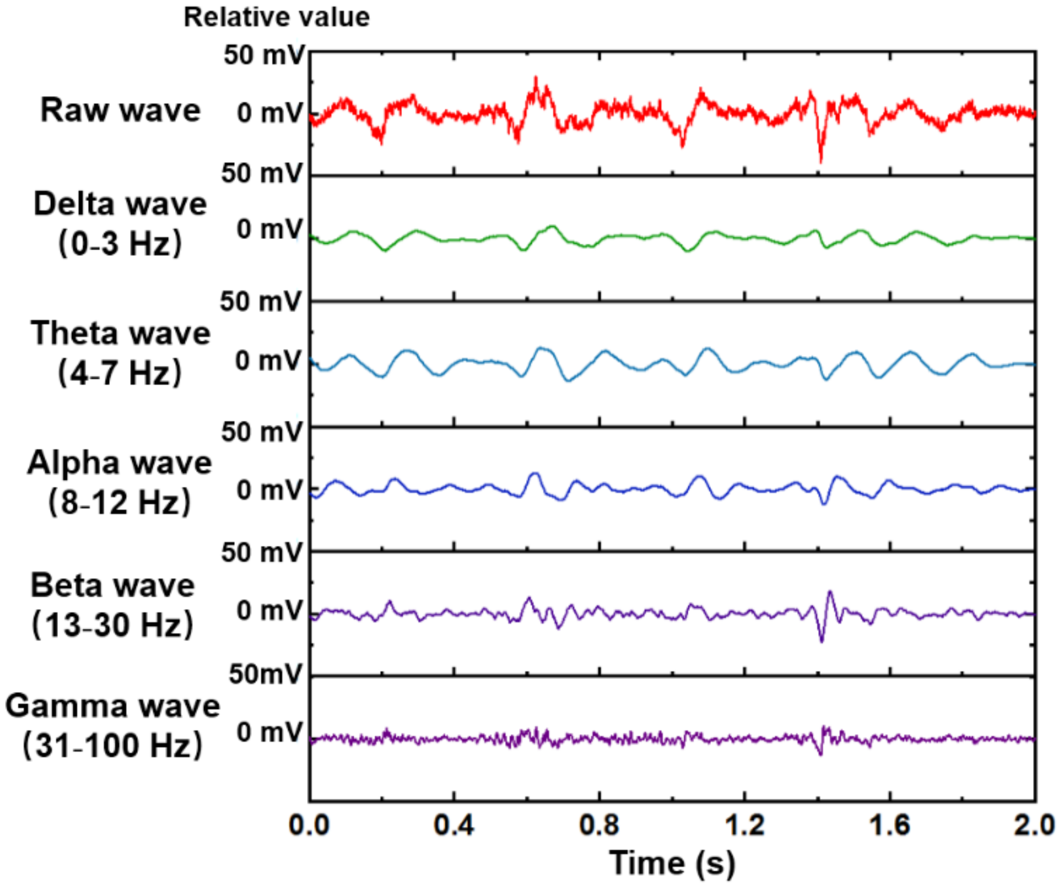

Fig. S17. Waveforms of the LFP signal in different frequency bands. From top to bottom are the raw wave, delta (0–3 Hz) wave, theta (4–7 Hz) wave, alpha (8–12 Hz) wave, beta (13–30 Hz) wave, and gamma (31–100 Hz) wave, respectively.

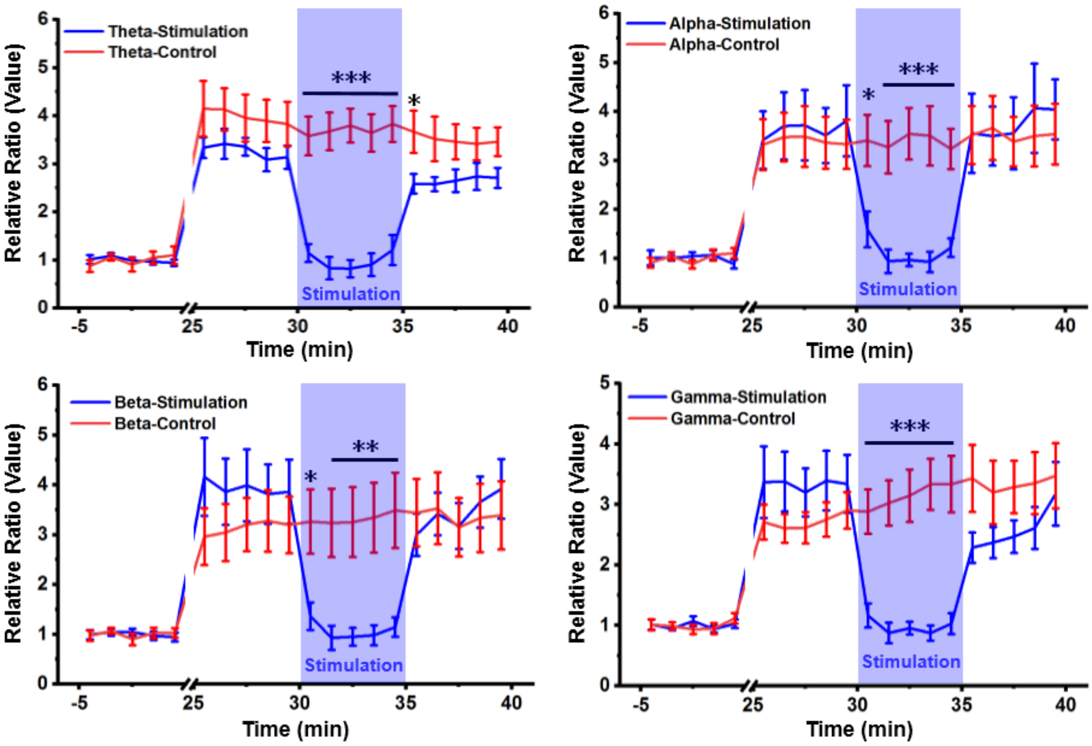

Fig. S18. The comparison of power spectrum changes in theta, alpha, beta, and gamma wave between the control group (n = 8) and the stimulation group (n = 8) after formalin injection. The power spectrum is calculated by the average of each minute, and ratio is processed by the average baseline of the first five minutes. All data are presented as mean ± SEM. *$P < 0.05$, **$P < 0.01$, ***$P < 0.001$, vs. control group.

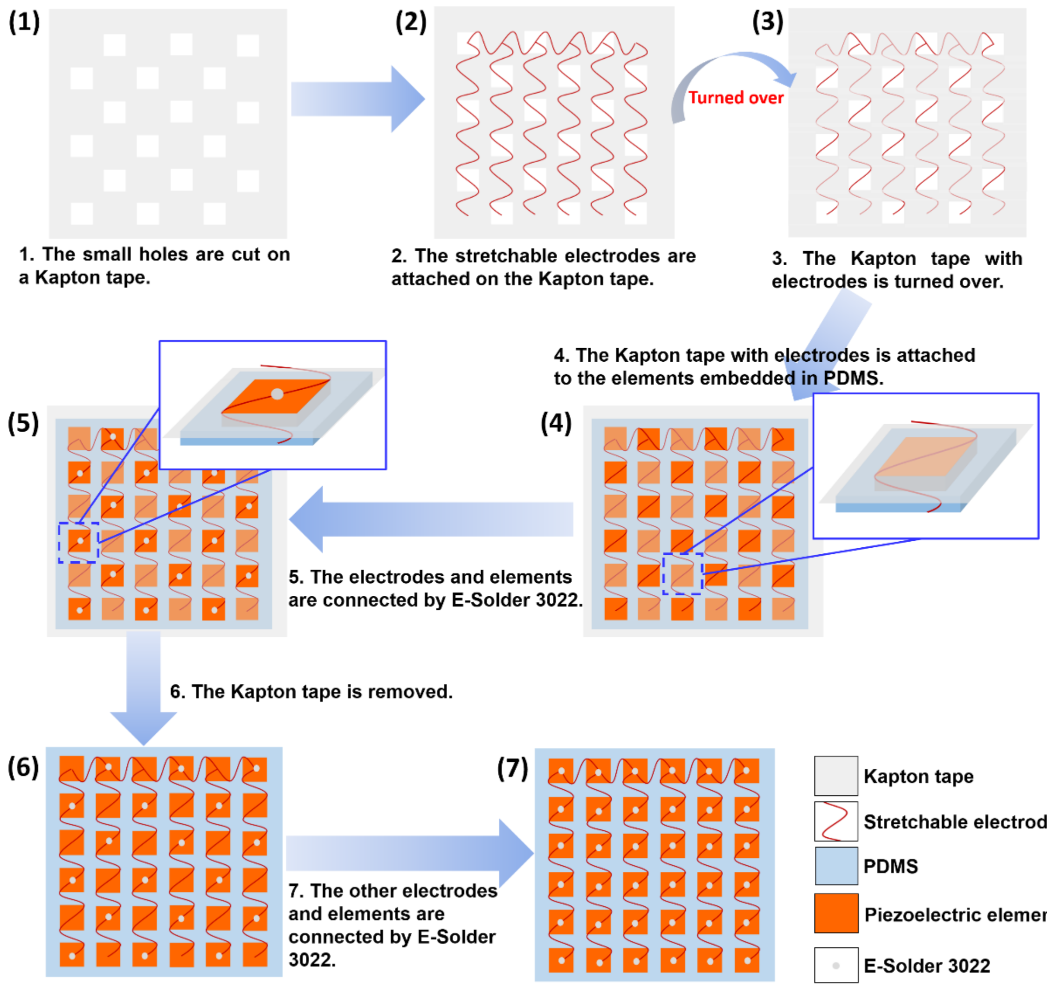

Fig. S19. Schematic diagram of the method for connecting the stretchable electrodes with piezoelectric elements.

Table S1. Comparison of representative wireless power transmission technologies.

Technology	Ref.	Energy source | frequency	Output | Input	*In vivo* or *in vitro*	Advantages	Drawbacks
Electromagnetic	(*25*)	RF signal | 6.78 MHz	~ 3.7 V |12.5 W	*in vivo*	High output power	Low threshold; electromagnetic interference; complexity in fabrication
	(*26*)	RF signal | 1.6 GHz	0.45 mW | 800 mW	*in vitro*		
	(*27*)	RF signal | 2.34 GHz	~ 100 μW | 2 W	*in vivo*		
Piezoelectric	(*20*)	Magneto | 250 − 400 kHz	2 mW | 7 W	*in vivo*	High output power	Complexity in fabrication
	(*21*)	Ultrasound | 1.85MHz	~400 μA | ~ 692 mW/cm^2	*in vivo*	High penetration depth; high safety threshold	Low output power; long-term charging
Triboelectric	(*28*)	Ultrasound | 20 kHz	98.6 μW |1 W/cm^2	*in vitro*	High output power	Complexity in fabrication
	(*29*)	Peristalsis stomach | 0.05 Hz	100 mV | −	*in vivo*	Regenerative	Low output power; long- term charging
	(*30*)	Body motion | −	[B] 360 mV | 0.4 m/s	*in vivo*		
Electrostatic	(*31*)	Ultrasound | 25 kHz	24.7 nW | −	*in vitro*	−	Low output power; few implantation
	(*32*)	Heart beat | 1−2 Hz	20 μJ | −	*in vitro*	Regenerative	
	(*33*)	Ultrasound | 1 MHz	27 mV | 1.2 W/cm^2	*in vitro*	−	
Bio-Fuel cell	(*34*)	Enzymatic catalysis | −	0.42 V| 16 μW/mL	*in vivo*	Recycle materials	Low output power
	(*35*)	Enzymatic catalysis | −	~4.4 μW | PH = 6.2	*in vitro*		
Thermoelectric	(*36*)	Temperature gradient | −	645 μW | ΔT = 3.5 K	*in vivo*	Regenerative; unlimited lifetime	Low instantaneous output power
	(*37*)	Temperature gradient | −	1 μW | Δ T = 5 K	*in vitro*		
Photovoltaic	(*38*)	Near-infrared light | −	~10.3 mW | ~ 3.3 W/cm^2	*in vivo*	Regenerative	Low instantaneous output power; long- term charging; low penetration depth
	(*39*)	Light | −	0.27 V | 298.15 K	*in vitro*		
This work	−	Ultrasound | 1MHz	280 μW | 212 mW/cm^2 7.7 V | 212 mW/cm^2	*in vivo/ in vitro*	High penetration depth; high safety threshold; high output power; good controllability	−

[B] Estimated based on published data.

Table S2. Comparison of representative piezoelectric materials for PUEH.

Ref.	Materials	Size (mm^2)	Frequency	Input condition	Medium	Output condition	Output power density	η
(*41*)	PVDF	[B]300	14 MHz	2.05 mW	In water	[B]load 64 KΩ	[B]76.7μW/cm^2	–
(*42*)	PZT	2.058	240 KHz	1 mW/cm^2	In water	load 50 Ω	3.75 μW/cm^2	[B]0.375%
(*43*)	PZT 1-3	[B]314	970 KHz	–	In air	load100 Ω	[B]60 mW/cm^2	–
(*44*)	PZT 1-3	[B]5402	350 KHz	65 mW/cm^2	In water	–	4.1 μW/cm^2	[B]0.063%
(*45*)	KNN 1-3	[B]1	304 KHz	[B]5.887 W/cm^2	In water	load 1 KΩ	45 mW/cm^2	[B]0.76%
This work	Sm-PMN-PT	36	1 MHz	20.3 W/cm^2	In water	load 1 KΩ	1.1 W/cm^2	5.4%

[B] Estimated based on published data.

The conversion coefficient (η) is defined as:

$$\eta = \frac{E_{out}}{E_{in}} \times 100\%,$$

where E_{out} is output energy and E_{in} is input energy.

Table S3. Comparison of representative wireless charging devices.

Ref.	(*25*)	(*21*)	(*29*)	(*34*)	(*36*)	(*38*)	**This work**
Principle of technology	Electromagnetic	Piezoelectric	Triboelectric	Bio-Fuel cell	Thermoelectric	Photovoltaic	Piezoelectric
Power type (implant)	RF antenna	Ultrasound	Peristalsis stomach	Enzymatic catalysis	Temperature gradient	Near-infrared light	Ultrasound
Implantable? (Fully or half)	Fully	Fully	Fully	Fully	Half	Fully	Fully
Animal type	Rat	Rat	Rat	Rabbit	Rat	Mice	Rat
Stimulation type	LED	Electrical	Electrical	Electrical	Electrical	LED	Electrical
Implantation site	Head	Leg	Surface of stomach	Abdomen	Head	Head / back	Head
Stimulus site	Brain	Sciatic nerve	Vagus	–	–	Brain	Brain
Stimulation effect	Activity control	Muscle activation	Weight control	–	–	Whisker movement	Analgesia
Carrier frequency	6.78 MHz	1.85 MHz	0.05 – 2 Hz	–	–	38 KHz	1 MHz
Stimulation frequency (Hz)	5 – 40 Hz	0–5,000 Hz	0.05 – 2 Hz	–	–	–	0–120 Hz
Stimulation frequency adjustable?	Yes	Yes	No	–	–	Yes	Yes
Operation control	Bluetooth	External ultrasound	Peristalsis stomach	Bluetooth	–	Modulated light	External ultrasound
Battery or rechargeable?	Yes	Yes	No	Yes	–	Yes	No
Immediate stimulation?	No	No	No	No	No	No	Yes
Verify biosafety?	Yes	No	Yes	Yes	No	No	Yes
Whole implant size (mm)	19 × 12 × 5	1.7 mm^3	16 × 12 × 2.5	–	83 mm^2	25 × 17 (large part)	13.5 × 9.6 × 2.1
Freely moving (y/n)	Yes	No	Yes	Yes	No	No	Yes
Implant weight (g)	1.4	0.0064	~ 0.8	–	–	–	0.7
Out performance (*in vivo*)	~ 3.7 V	50 µA – 400 µA	~ 200 µV	0.42 V	645 µW	~10.3 mW	400 µW (Max)
Instantaneous effective power (*in vivo*)	–	–	–	–	–	–	280 µW
Input power	12.5 W	~ 692 mW/ cm^2	N/A	16 µW/mL	ΔT– 3.5 K	~ 3.3 W/ cm^2	212 mW/cm^2

Table S4. Parameters of Sm-PMN-PT.

Parameters	Value
Piezoelectric coefficient d_{33}	4000 pC/N
Electromechanical coupling coefficient k_{33}	95%
Relative free permittivity $\varepsilon_{33}/\varepsilon_0$	13000
Dielectric loss tan δ	0.005
Thickness h	0.38 mm
Density ρ	8100 kg/m^3
Acoustic velocity c_p	4400 m/s
Acoustic impedance Z_a	36 MRayls

Table S5. Simulation parameters of ultrasound penetrating Skull (*51*).

Parameters	Value
Ultrasound frequency	0.5 MHz/1 MHz
Density of skin(g/cm^3)	1.15
Density of Skull(g/cm^3)	1.9
Density of Brain(g/cm^3)	1.03
Speed of Sound in Skin(m/sec)	1730
Speed of longitudinal waves in Skull(m/sec)	4080
Speed of shear waves in Skull(m/sec)	2800
Speed of Sound in Brain(m/sec)	1550
Attenuation in Skin[dB/(cm MHz)	1.84
Attenuation in Brain[dB/(cm MHz)]	0.8

Table S6. Parameters of ultrasound energy harvesters.

Ref.	UEH device	Size (mm^2)	Frequency	Input condition	Medium	Output condition C_s (μF)	T(s)	V_o(V)	$\bar{P}$(nW)
(*31*)	Omnidirectional UEH	[B]7.4	25 kHz	60 V	In air	1	15	0.86	24.7
(*44*)	PZT(1-3) PUEH	[B]5402	35 kHz	150 V	In water	1000	900	0.27	40
(*45*)	LF-PUEH	[B]1	3.4 kHz	100 V	In water	220	200	0.54	160.38
(*56*)	2-D MEMS UEH	[B]1	38.53 kHz	60 V	In air	1	15	[B]0.44	21. 4
(*57*)	3-D MEMS UEH	[B]6.25	36 kHz	100 V	In air	1	20	0.71	12.6
This work	Sm-PUEH	36	1 MHz	150 V	In water	1000	180	1.25	4270 ± 40

[B] Estimated based on published data.

The average charging power ($\bar{P}$) is calculated by the following formula (*31*):

$$\bar{P} = \frac{C_S {V_O}^2}{2T}$$

where f is the ultrasound working frequency, C_S is the capacitance, T is the charging time, and V_O is the effective output voltage.

Table S7. US waveform properties used in animals in this work

f (MHz)	C/P	PRF (Hz)	Pr (MPa)	I_{SPTA} (mW/cm^2)	MI	*Safe or not
1	400	50	0.65	212.25	0.65	safe
1	400	75	0.65	318.375	0.65	safe
1	400	100	0.65	424.5	0.65	safe
1	400	125	0.65	531	0.65	safe
1	400	150	0.65	636.75	0.65	safe

$$I_{SPTA} = \int \frac{P^2(t)}{Z_0} dt \times PRF$$

Where P is the instantaneous peak pressure; Z_0 is the characteristic acoustic impedance in Pa s/m, which is defined as $Z_0 = \rho c$; where ρ is the density of the medium, and c is the speed of sound in the medium (Skin:1.15g/cm^3,1730m/s in this work) (*72*).

$$MI = \frac{p_r}{\sqrt{f}}$$

wherein p_r is the peak negative pressure of the US in MPa, and f is the center frequency of the US transducer in MHz (*72*).

***Safe or not**: According to the Food and Drug Administration (FDA)'s regulation, the safety threshold of ultrasound in the human body is 720 mW/cm^2 (*23*).

Note S1: Theoretical analysis of excellent power output of Sm-PUEH device

In this work, the width-to-thickness ratio of the single element in this device we designed is about 2.63 (1000 μm / 380 μm ≈ 2.63). Based on the output power theory of a piezoelectric harvester in thickness-stretch mode of a plate (*48*), we explore the huge advantages of output power based on Sm-PMN-PT single crystal.

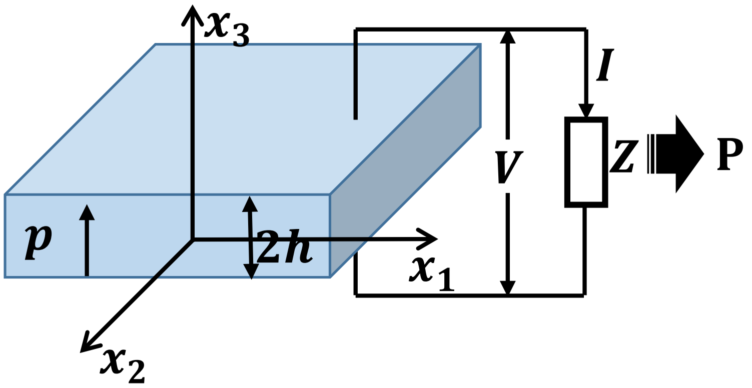

Fig.Note-S1. Schematic diagram of a plate in thickness-stretch mode, where $\boldsymbol{p}$ is the Stress amplitude, $\boldsymbol{Z}$ is Load, I is output current, $\boldsymbol{V}$ is the output voltage and **P** is the output power. Among them, $T_{33} = pexp(i\omega t)$, and $T_{31} = T_{32} = 0$.

According to the governing formulas of three-dimensional linear piezoelectricity (*47*), the formulas of the plate can be obtained as follows:

$$T_{11} = T_{22} = c_{13}u_{3,3} + e_{31}\emptyset_{,3}; \quad (1)$$

$$T_{33} = c_{33}u_{3,3} + e_{31}\emptyset_{,3}; \quad (2)$$

$$D_3 = e_{33}u_{3,3} - \varepsilon_{33}\emptyset_{,3}; \quad (3)$$

$$S_{33} = u_{3,3}; \quad (4)$$

$$E_3 = -\emptyset_{,3}; \quad (5)$$

where u the mechanical displacement vector, T is the stress tensor, S is the strain tensor, E is the electric field vector, D is the electric displacement vector, and $\emptyset$ is the electric potential; c, e, and ε are the elastic, piezoelectric, and dielectric coefficient.

By solving the partial differential formulas of the above formula (1), (2), (3), (4), (5), it can be obtained:

$$\boldsymbol{I} = i\omega p\frac{\varepsilon_{33}}{e_{33}}\frac{1}{\left(1+\frac{1}{k_{33}^{2}}\right)}\frac{1}{\left(1+\frac{Z}{Z_0}\right)\xi h\cot(\xi h) - \bar{k}_{33}^{2}} \quad (6)$$

$$\boldsymbol{V} = i\omega p\frac{\varepsilon_{33}}{e_{33}}\frac{1}{\left(1+\frac{1}{k_{33}^{2}}\right)}\frac{Z}{\left(1+\frac{Z}{Z_0}\right)\xi h\cot(\xi h) - \bar{k}_{33}^{2}} \quad (7)$$

$$\mathbf{P} = \frac{1}{2}|I|^2 Re\{Z\} = \frac{\omega^2 p^2}{2}\frac{\varepsilon_{33}|\bar{k}_{33}^{2}|}{|\bar{c}_{33}|}Re\{Z\}\left|\frac{1}{\left(1+\frac{Z}{Z_0}\right)\xi h\cot(\xi h) - \bar{k}_{33}^{2}}\right|^2 \quad (8)$$

where ${k_{33}}^2 = \frac{{e_{33}}^2}{\varepsilon_{33} c_{33}}$, ${\bar{k}_{33}}^2 = \frac{{k_{33}}^2}{1+{k_{33}}^2}$, $\bar{c}_{33} = c_{33}(1 + {k_{33}}^2)$, $\xi^2 = \frac{\rho}{c_{33}(1+{k_{33}}^2)}$. In the above formulas, p is the acoustic pressure amplitude applied on the upper surface of the harvester, Z is the load and $\mathrm{Z_0}$ is the internal resistance.c_{33}, $\mathrm{e_{33}}$ and ε_{33} are the effective elastic coefficient, the piezoelectric coefficient, and dielectric coefficient; h, ρ, ω and ξ are the thickness, the effective mass density, angular frequency, and wave number.

Only considering the material parameters, we simplify the above formula (8):

$$\mathrm{P} \propto \frac{\varepsilon_{33}}{c_{33}} \frac{1}{(k_{33} + \frac{1}{k_{33}})^2} \tag{9}$$

The value of k_{33} is in the range of 0–1, so the formula $\frac{1}{(k_{33}+\frac{1}{k_{33}})^2}$ is a monotonically increasing function. Therefore, according to the formula (9), a larger dielectric coefficient(ε_{33}), and a larger electromechanical coupling coefficient (k_{33}) help to increase the output power. Of course, the maximum output power can be obtained at the resonance frequency.

In this work, Sm-PUEH device we designed works at the resonant frequency (1MHz, **Fig. S7**), and the Sm-PMN-PT single crystal has a larger relative free permittivity and electromechanical coupling coefficient ($\varepsilon_{33}/\varepsilon_0 = 13000$, $k_{33} = 95\%$, **Table S4**).

Captions for Supplementary Movies

Movie S1

High voltage output (80 Vpp) of Sm-PUEH device under pulse ultrasound (US–1 MHz, 2.5 MPa).

Movie S2

The voltage output of Sm-PUEH device with incident angle of 30° under pulse ultrasound (US–1 MHz, 2.5 MPa).

Movie S3

The voltage output of Sm-PUEH device in the bent state under pulse ultrasound (US–1 MHz, 2.5 MPa).

Movie S4

The charging of a capacitor (470 μF) by Sm-PUEH device under pulse ultrasound (US–1 MHz, 1000 c/p, PRF = 100 Hz, 2.5 MPa).

Movie S5

Lighting of 55 blue LEDs with "***HUST***" pattern after three 220 μF capacitors charged by Sm-PUEH device under pulse ultrasound (US–1 MHz, 1000 c/p, PRF = 100 Hz, 2.5 MPa) for five minutes.

Movie S6

Instant lighting of one blue LED connected with a 220 uF capacitor in parallel charged by Sm-PUEH device under pulse ultrasound (US–1 MHz, 1000 c/p, PRF = 100Hz, 2.5 MPa).

Movie S7

The output voltage of Sm-PUEH device in pork tissue under pulse ultrasound (US–1 MHz, 0.65 MPa).

Movie S8

Behavioral experiment of analgesia application. The fully implanted Sm-PUEH device achieves analgesia under pulse ultrasound (US–1 MHz, 400 c/p, PRF = 50 Hz, 0.65 MPa).

Movie S9

Biocompatibility study of Sm-PUEH device after long-term implantation.